CSIRO PUBLISHING

Australian Journal of Physics

Volume 52, 1999

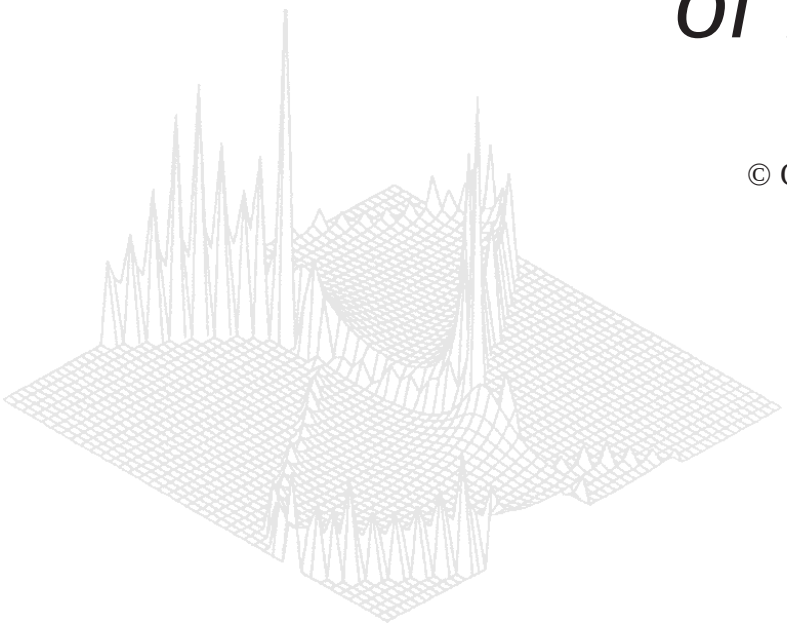

A journal for the publication of
original research in all branches of physics

www.publish.csiro.au/journals/ajp

All enquiries and manuscripts should be directed to
Australian Journal of Physics
CSIRO PUBLISHING
PO Box 1139 (150 Oxford St)
Collingwood Telephone: 61 3 9662 7626
Vic. 3066 Facsimile: 61 3 9662 7611
Australia Email: peter.robertson@publish.csiro.au

Published by **CSIRO** PUBLISHING
for CSIRO Australia and
the Australian Academy of Science

Aust. J. Phys., 1999, **52**, 545–54

Multiple Ionisation and Fragmentation of Molecules*

B. Siegmann, U. Werner and H. O. Lutz

Fakultät für Physik, Universität Bielefeld,
D-33615 Bielefeld, Germany.

Abstract

The multiple ionisation and dissociation of molecules, e.g. H_2, N_2, H_2O, CH_4 and C_{60}, by fast ions was studied using a position- and time-sensitive multi-particle detector. The data obtained allow a clear separation of various reaction channels. Of special interest are the 'Coulomb explosion' processes like $N_2 \longrightarrow N^{q+} + N^{n+}$ or $H_2O \longrightarrow H^+ + H^+ + O^{n+}$. For these reactions the coincident measurement of the momenta of correlated fragment ion yields a *kinematically complete* image of the molecular break-up process, and the fragmentation energy as well as angular correlations can be derived for each individual event. In the case of H_2 as target molecule the CE model describes the fragmentation energy rather well, whereas in the case of more complex molecules, e.g. N_2, CO and CH_4, the simple CE model is insufficient to explain the measured energy and angular spectra. Better agreement was achieved with *ab initio* MCSCF calculations which take into account several molecular states of the fragmenting highly charged molecular ion.

1. Introduction

The ion-induced fragmentation of molecules is a process of fundamental importance in various areas of science ranging from the physics and chemistry of upper planetary atmospheres (Kirby 1993) to the understanding of radiation damage in biological tissue. In contrast to studies of the molecular break-up by electron bombardment, the ion-impact induced fragmentation has received comparatively little attention. Experiments in which *all* fragment ions emitted after a particular collision are detected in coincidence can not only provide valuable information about the charge state and potential energy surface of the intermediate multiply-charged molecular ion, but they also shed light on the excitation and fragmentation dynamics. Most work so far has concentrated on the observation of individual reaction products without further attention to the correlated behaviour of the remaining fragments (Latimer 1993, and references therein). Exceptions can be found in dissociation studies of some diatomic molecules where the correlation of both fragments has been studied in detail (e.g. de Bruijn and Los 1992; Folkerts *et al.* 1997) and in the Coulomb explosion studies of molecular ions (Vager and Kanter 1988). This latter technique is of

* Refereed paper based on a contribution to the Australia–Germany Workshop on Electron Correlations held in Fremantle, Western Australia, on 1–6 October 1998.

 10.1071/PH98089 0004-9506/99/030545$05.00

particular interest since it allows a *kinematically complete* study of molecular fragmentation. In the work to be reported here we use a similar approach to establish coincidences between low-energy fragments of a neutral molecule. The application of a time- and position-sensitive multi-particle detector allows the measurement of the correlated momentum vectors of several fragments. In the special case where all fragments from a particular break-up are detected, a kinematically complete analysis of the dissociation process is possible.

2. Experimental Set-up

Collimated beams of 5–350 kV H^+, He^+, Ar^{q+}, and 742 keV O^{7+} projectiles interact with a molecular gas target. The slow ions and electrons generated in the collision process are separated by a homogeneous electric field of 100–300 $V\,cm^{-1}$. Electrons are detected in a channeltron at one side of the interaction region; positive ions are accelerated towards the time- and position-sensitive multi-particle detector (Becker *et al.* 1994) at the other side (Fig. 1). After passing a field-free time-of-flight region the ions are post-accelerated to a few keV to increase the detection efficiency.

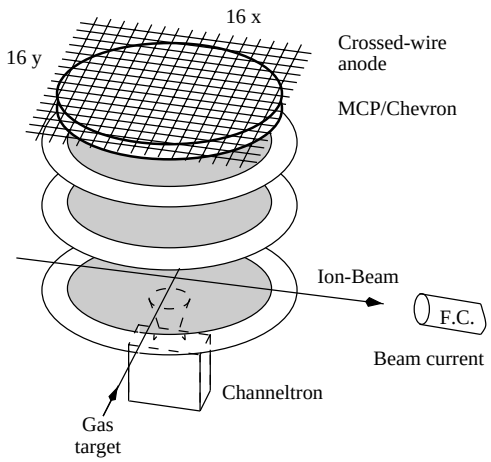

Fig. 1. Geometry of the fragmentation experiment.

The time- and position-sensitive detector is based on microchannel plates in combination with an etched crossed-wire structure consisting of independent x- and y-wires. If an electron cloud from the plates hits at a crossing of two wires, coincident pulses on the wires are generated and registered by the time-to-digital converter (TDC) which is the central part of the detector electronics. We use a special multi-hit TDC module which was developed in our group. The system is located on a VMEbus-card and has 32 channels with a time range of 17 μs and a typical resolution of 270 ps. The TDC is triggered by an electron pulse from the channeltron and the individual channels are stopped by the ion signals. Thereby, for each positive fragment the position (x_i, y_i) on the detector and the time-of-flight t_i relative to the start electron are recorded. Although there are position-sensitive detectors with higher positional resolution [e.g. wedge-and-strip (Martin *et al.* 1981) or resistive anodes (Firmani *et al.* 1982)] our system has one major advantage: as a consequence of the crossed-wire structure the detector is capable of resolving particles which arrive 'at the same time' on different wires.

This 'zero deadtime' feature is particularly useful to study the fragmentation of more complex molecules like CH_4 or even C_{60}, where several correlated fragments with equal masses occur (Werner *et al.* 1998).

The present experimental set-up is sensitive to all reaction channels resulting in at least one electron and one or more positive ions, whereas pure capture reactions such as $He^+ + N_2 \longrightarrow He + N_2^+$ are not observable. Thus relative cross sections for the production of selected ions (e.g. N_2^+, N^{q+} in collisions with N_2) and special processes (e.g. N_2 decaying to $N^{p+} + N^{q+}$) can be obtained. Furthermore, if all fragments of a particular break-up are detected, information about the fragmentation dynamics as well as the molecular structure can be derived.

3. Diatomic Molecules

The simplest and most frequently studied molecular target is H_2. In our current set-up only positively charged fragments are detected; the reaction channels of interest are therefore:

$He^+ + H_2 \longrightarrow$	$He^+ + H_2^+ + e^-$	ionisation	(1)
	$He^+ + H_2^{+*} + e^-$	dissociative ionisation	(2)
	$\rightarrow H^* + H^+$		
	$He^+ + H^+ + H^+ + 2e^-$	double ionisation	(3)
	$He + H_2^+$	capture	(4)
	$He + H_2^{+*}$	dissociative capture	(5)
	$\rightarrow H^* + H^+$		
	$He + H^+ + H^+ + e^-$	capture and ionisation	(6)
	$He^- + H^+ + H^+$	double capture.	(7)

The TDC system is triggered by an electron emitted during the collision; consequently the detector is sensitive to processes (1)–(3) and (6). Of special interest among these various reaction channels are those fragmentations leading to coincident proton pairs (process 3 and 6); these are widely called 'Coulomb explosions'. A simultaneous break-up into positive fragment ions suggests the application of the simple Coulomb-explosion (CE) model where the dynamics are governed by the strong mutual repulsion of the generated positive ions, and the kinetic energies and emission angles may be computed by assuming Coulomb forces acting between point charges as a first approximation. In this picture (at least for the short collision times under consideration) the result of the calculation is independent of the details of the ionisation process.

Fig. 2 shows the total kinetic energy distribution of coincident fragment ions from collisions of 200 keV He^+ with H_2 and N_2. The H_2 data are in good agreement with a Franck–Condon calculation (McCulloh 1968) assuming a Coulomb-explosion process. The situation changes in the case of more complex diatomic molecules like N_2. As a typical example Fig. 2*b* shows the prediction of a point-charge CE model in comparison with the kinetic energy distribution of coincident $N^+ + N^+$ fragment ions. The agreement between experimental data and the CE model is comparatively poor. The model overestimates the energy release, and the predicted width of the distribution is too small. The shape of the energy spectrum (Fig. 3) shows a distinct dependence on the projectile energy

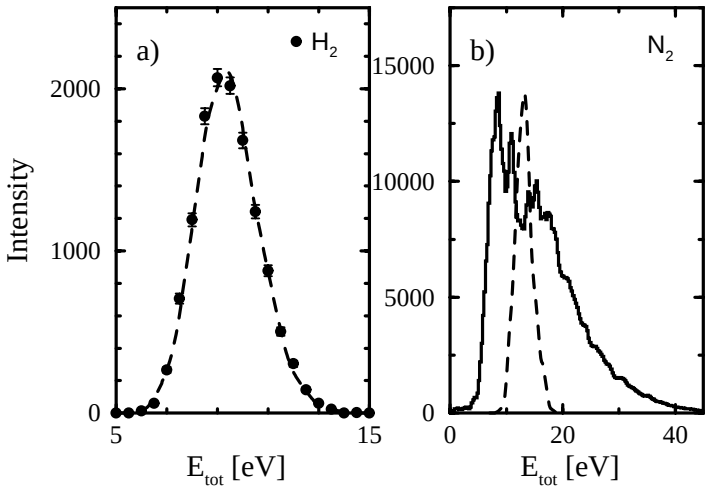

Fig. 2. Total kinetic energy of coincident fragments in collisions with 200 keV He^+: (*a*) $H_2 \longrightarrow H^+ + H^+$ and (*b*) $N_2 \longrightarrow N^+ + N^+$. The dashed lines are the predictions of the Coulomb explosion model.

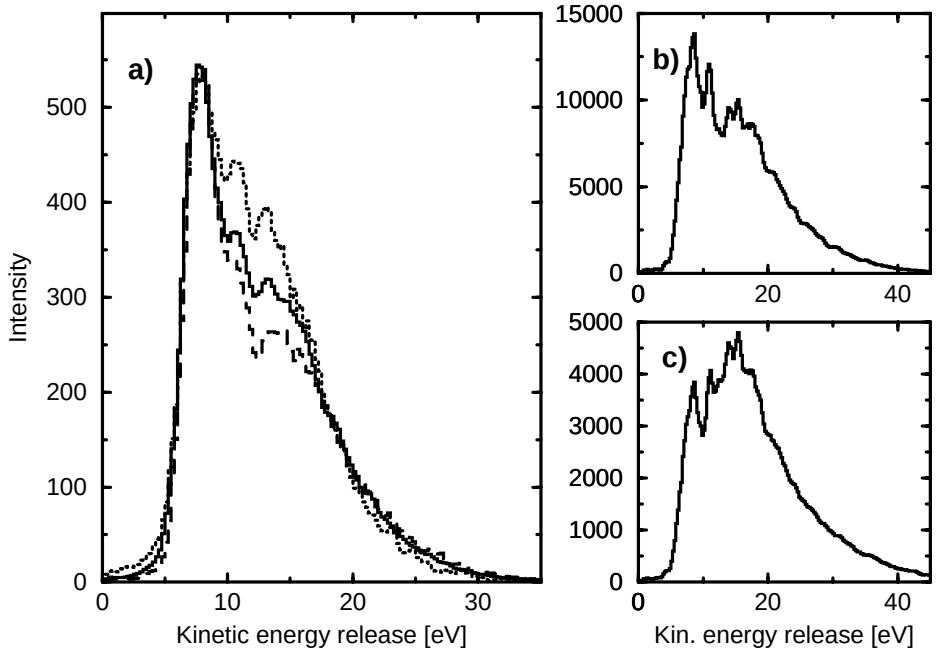

Fig. 3. Total kinetic energy of coincident N^++N^+ fragments in collisions of (*a*) (···) 5 keV, (—-) 10 keV, and (- - -) 25 keV H^+ on N_2, (*b*) of 200 keV He^+ on N_2 and (*c*) of 200 keV Ar^{2+} on N_2.

(especially at small projectile energies) and on the projectile type (Werner *et al.* 1997*b*) which is inconsistent with a point charge CE model. Several competing processes which all result in two correlated N^+ ions must be involved to explain this behaviour. In this picture the dependence on the projectile energy and type can be attributed to different populations of the excited states of the intermediate fragment ions: in general many different states of e.g. $(N_2)^{(p+q)+}$ exist which finally result in $N^{p+} + N^{q+}$ fragments, whereas in the case of H_2 only one potential curve describes the final $H^+ + H^+$ products. This is qualitatively consistent with the work of Edwards and Wood (1982) who studied the $N^+ + N^+$ production in collision of 1 MeV He^+ with N_2. To explain this kinetic energy distribution they postulated three dissociative states of N_2^{2+} with characteristic energy releases of $7{\cdot}8$, $10{\cdot}2$ and $14{\cdot}8$ eV.

To account for the most dominant reaction channels we used the MOLPRO Code* (Werner *et al.* 1995*a*; Werner and Knowles 1985) for an *ab initio* multi-configuration self-consistent field computation (MCSCF) of the lowest molecular states of the intermediate $(N_2)^{2+}$ ion. Not all of these states are purely repulsive; some show deep minima which correspond to (meta-)stable states. The total kinetic energy and angular distributions were computed by Monte–Carlo techniques assuming a Franck–Condon transition from the molecular ground state to the particular dissociation state. A comparison of the measured energy spectra to the MCSCF-prediction shows reasonable agreement (Fig. 4).

The fragments in a diatomic molecule emerge in the direction of the molecular axis so that the initial orientation of the molecule can be derived from the measured velocity vectors. In the data analysis the direction of the molecular axis was derived from the measured positions and times for each electron–ion–ion coincidence. Fig. 5 shows the measured intensity as a function of the angle θ between the molecular axis and the projectile beam. As an example, we present the results for 200 keV He^+ collisions with N_2 (Werner *et al.* 1997*b*). The alignment dependence for the e.g. triply ionised $(N_2)^{3+}$ was derived from the angular distribution for the reaction $(N_2)^{3+} \rightarrow N^{2+} + N^+$; in the case of $(N_2)^{4+}$ there are contributions of the channels N^+N^{3+} and $N^{2+}N^{2+}$. If the ionisation cross section is independent of the orientation of the molecule, the number of dissociation events is proportional to $\sin\theta$ and the probability-density is $f(\theta)=\frac{1}{2}\sin\theta$ (dotted line). In case of e.g. He^+ impact, our data clearly show—at least for four- and fivefold ionisation—significant deviations from the sine distribution, i.e. significant alignment effects. The alignment dependence for N^{2+}–N^{3+} shows a pronounced minimum at the perpendicular orientation. The origin of this strong orientation effect is due to the anisotropy of the electron density distribution (Wohrer and Watson 1993; Werner *et al.* 1997*a*) and the related anisotropy of the energy deposition along a trajectory. For a given ion trajectory the transferred energy and therefore the multiple ionisation probability depends crucially on the molecular orientation. In order to remove several electrons a large energy deposition is needed. When a diatomic molecule is oriented along the beam the probability of a large energy deposition is greater than for an

* MOLPRO is an *ab initio* program written by H. J. Werner and P. J. Knowles with contributions from J. Almlöf, R. Amos, S. Elbert, K. Hampel, W. Meyer, K. Peterson, R. Pitzer and A. Stone.

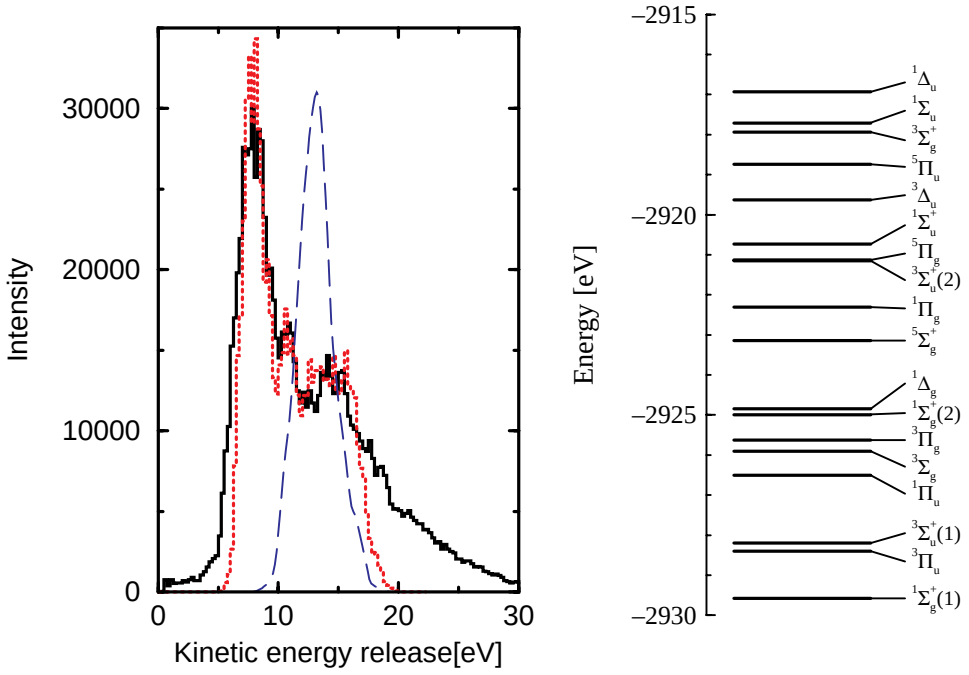

Fig. 4. (*left*) Total kinetic energy of coincident N^+N^+ fragments from collisions with 300 keV H^+. The dotted curve is a simulation based on the calculated MCSCF-potential curve; the dashed line is the prediction of the CE model. (*right*) MCSCF energies of calculated $(N_2)^{2+}$ levels at an equilibrium distance of the N_2^+ ground state.

orientation perpendicular to the beam, because the projected electron density 'seen' by the projectile is larger for trajectories close to the molecule axis.

In contrast to H^+ and He^+ collisions with N_2, an analysis of Bi^{25+} and Bi^{57+} data revealed no striking deviations from an isotropic distribution (Brinkmann *et al.* 1998). For singly charged projectiles multiple ionisation mainly occurs at small impact parameters where the energy transfer is sensitive to the shape of the electron density. In collisions with swift highly charged ions, the ionisation may take place at larger distances. Therefore, the sensitivity to the orientation is reduced and the alignment effect disappears.

4. Triatomic Molecules

As pointed out above, in general many different combinations of reaction products occur in collisions with triatomic molecules. As a first example we consider the fragmentation of H_2O which is fairly simple since it consists only of two kinds of atoms which can be easily distinguished due to their large mass difference. Furthermore, only the O-atom may occur in different charge states. Among the various reaction channels occurring in ion–water collisions we concentrate on complete fragmentation of the type

$$\begin{aligned} X^{p+} + H_2O \longrightarrow\ & H_2O^{(q+2)+} + X^{(p-m)+} + (q+2-m)e^- \\ & \rightarrow H^+ + H^+ + O^{q+} \end{aligned}$$

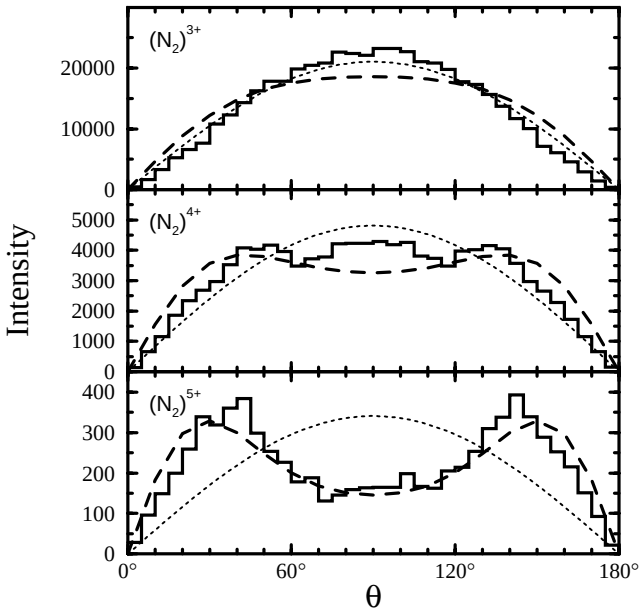

Fig. 5. Alignment dependence for the multiple ionisation of N_2 molecules in collisions with 200 keV He^+. Histograms shows the experimental results, dashed curves are the results of the theoretical calculations within the statistical-energy-deposition model (Werner *et al.* 1997), and dotted curves show the $\sin\theta$ distribution. All of the curves are normalised to the same area.

where $q+2-m \geq 1$. In the experiment these events appear as 4-fold coincidence between an electron and the three positive fragment ions. In collisions with H^+ and He^+ we observed processes with $q \leq 2$. A useful tool for the identification and separation of two-particle coincidences is a coincidence map. The coincidence maps in Fig. 5 give an overview on the two- (Fig. 6*a*) and the three-particle events (Fig. 6*b*) detected in collisions with 742 keV O^{7+} on H_2O. The three-particle map shows those two-particle events which are detected in coincidence with a H^+ fragment.

In the case of a complete fragmentation process the conditions for a kinematically complete description are fulfilled and the fragmentation dynamics may be analysed in terms of three independent parameters which are derived from the measured velocity vectors. A practical choice of characteristic variables consists of the kinetic energy release and the angles χ and θ_v in velocity space (Werner *et al.* 1995*a*); χ is the angle between the $H^+ - H^+$ relative velocities v_{HH} and the velocity of the O^{q+}-ion v_{O}, and θ_v is the angle between the two O^{q+}–H^+ relative velocities. These velocity-space coordinates contain information about the geometric structure of the molecule at the instance of fragmentation. The angle χ indicates that in case of H_2O the molecule breaks up simultaneously into three positive fragments (Werner *et al.* 1995*a*). However, again in contrast to a simple CE picture, and similar to the N_2 results, the shapes of the measured angular distributions (θ_v spectrum) and the total kinetic energy clearly change with the projectile type. Several competing processes which all result in three positive fragment-ions must be involved to explain this behaviour.

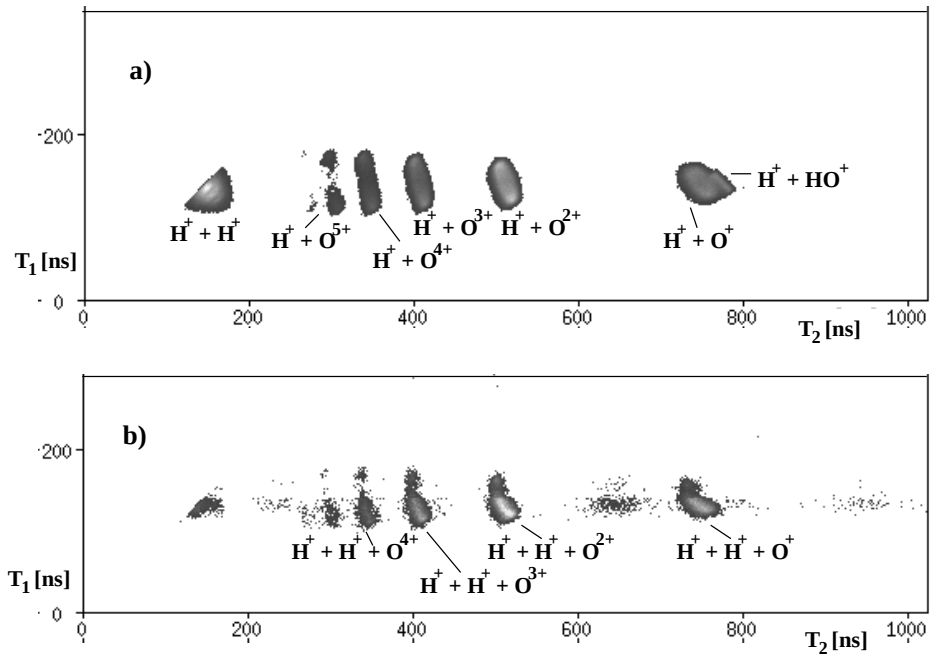

Fig. 6. Correlation map of H_2O in collisions with 742 keV O^{7+}: (*a*) Coincidence spectrum of two-particle events (flight time T_1 of the first fragment-ion versus flight time T_2 of the second fragment). (*b*) Coincidence spectrum of three-particle events (two-particle events which are detected with a H^+ ion).

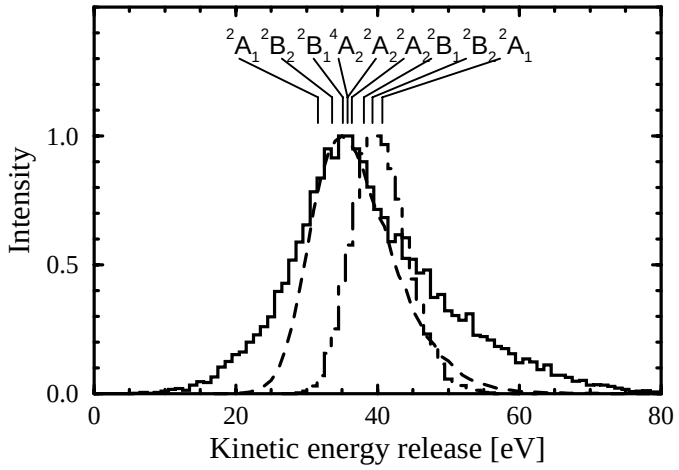

Fig. 7. Total kinetic energy distribution of coincident $H^+ - H^+ - O^+$ fragments from collisions of H_2O with 250 keV He^+ (—-). The dashed curve is the result of an *ab initio* MCSCF-calculation taking into account the indicated molecular states of H_2O^{3+} which are labeled by their symmetries; the prediction of a point charge Coulomb explosion model is shown by the dashed histogram.

A computation of the nine lowest potential surface of the intermedial $(H_2O)^{3+}$ molecular ion indeed shows a significantly improved agreement with the measured spectra. Even better agreement was achieved in collisions with highly charged O^{7+}-ions (Werner *et al.* 1995*b*) where excited states are seen to be less important (see Fig. 7).

5. Polyatomic Molecules

Even more complicated is the situation for larger molecules such as CH_4 or C_{60}. In the case of CH_4 complete fragmentations in two ($CH_3^+ + H^+$ and $CH^{2+} + H_2^+$), three ($CH_2^+ + 2H^+$ and $CH^+ + H^+ + H_2^+$), and five ($C^{q+} + 4H^+$) fragments have been observed. Whereas the CE model allows at least a qualitative explanation of the measured kinetic energies for the process $CH_4 \longrightarrow C^{2+} + 4H^+$, it has conceptual problems to explain the fragmentation into two or three fragments (see Fig. 8). In particular, the assumption of point charges is unsuitable for an understanding of the occurrence of channels like $CH_4 \longrightarrow CH_2^+ + H_2^+$. Furthermore, there are hints that stepwise fragmentation processes play a role in some reaction channels.

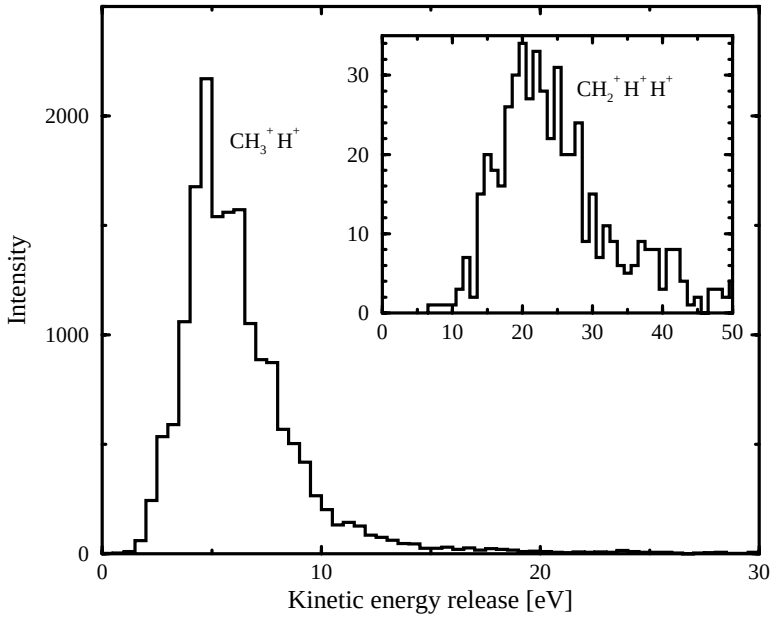

Fig. 8. Total kinetic energy distribution of coincident CH_3+H^+ and coincident $CH_2+H^++H^+$ fragment ions (inset) from collisions of 742 keV O^{7+} on CH_4.

In the case of C_{60} a complete study of multi-fragmentation is not possible since too many fragments had to be detected, with correspondingly low detection efficiency of the complete ensemble. Nevertheless, interesting information on the fragmentation process can be gleaned even in such complex situations (Werner *et al.* 1998). For example, the 'fission' into $C_{60-2n}^{q+} + C_{2n}^+$ and multiple fragmentation into small charged fragment ions are observed in the coincidence spectra, besides the well known features of multiple ionisation and evaporation

of C_{2n}. The fragmentation patterns show a striking dependence on the projectile type (Reinköster *et al.* 1998), whereas the influence of the collision energy is comparatively weak in an energy range of 50–300 kV.

Most collisions with H^+ and D^+ lead to ionisation or fragment fullerenes C_{60-2n}^{q+}: multi-fragmentation is almost negligible and the low mass region in the correlation spectra is dominated by contributions from residual gas. For He^+ impact an increased abundance of small C_n^+ fragments is observed, whereas for heavier projectiles like Ar^{q+} the small C_n^+ ions clearly dominate.

In summary, we have studied the fragmentation of small molecules in collisions with fast (5–350 keV) H^+, He^+, Ar^{q+}, and 742 keV O^{7+} projectiles. In many cases, the applied technique allows an even *kinematically complete* study of the molecular break-up process, and the dissociation energy as well as angular correlations can be derived. If electrons remain in the highly ionised molecular complex, the observed fragmentation patterns are found to depend strongly on the projectile type and energy. This is inconsistent with a simple CE model. A better agreement was achieved with *ab initio* MCSCF calculations.

Acknowledgments

The authors wish to thank Prof. R. Morgenstern and his group for their support during the measurements with the O^{7+} ions at the ECR ion-source at the KVI in Groningen, as well as for many stimulating discussions. This work was supported by the Gesellschaft für Schwerionenforschung (GSI) and the Deutsche Forschungsgemeinschaft (DFG).

References

Becker, J., Beckord, K., Werner, U., and Lutz, H. O. (1994). *Nucl. Instrum. Methods* A **337**, 409.

Brinkmann, U., Reinköster, A., Siegmann, B., Werner, U., Lutz, H. O., and Mann, R. (1999). *Phys. Scripta*, in press.

de Bruijn, D. P., and Los, J. (1982). *Rev. Sci. Instrum.* **53**, 1020.

Edwards, A. K., and Wood, R. M. (1982). *J. Chem. Phys.* **76**, 2938.

Firmani, C., Ruiz, E., Carlson, C. W., Lampton, M., and Paresce, F. (1982). *Rev. Sci. Instrum.* **53**, 570.

Folkerts, H. O., Bliek, F. W., deJong, M. C., Hoekstra, R., and Morgenstern, R. (1997). *J. Phys.* B **30**, 5833; 5849.

Kirby, K. P. (1993). *In* 'The Physics of Electronic and Atomic Collisions', Proceedings of the XVIII ICPEAC Conference (Eds T. Andersen *et al.*), pp. 48–58 (AIP Press: New York).

Latimer, C. J. (1993). *Adv. At. Mol. Opt. Phys.* **30**, 105.

McCulloh, K. E. (1968). *J. Chem. Phys.* **48**, 2090.

Martin, C., Jelinsky, P., Lampton, M., Malina, R. F., and Anger, H. O. (1981). *Rev. Sci. Instrum.* **52**, 1067.

Reinköster, A., Werner, U., and Lutz, H. O. (1998). *Europhys. Lett.* **43**, 653.

Vager, Z., and Kanter, E. P. (1988). *Nucl. Instrum. Methods* B **33**, 98.

Werner, H. J., and Knowles, P. J. (1985). *J. Chem. Phys.* **82**, 5053.

Werner, U., Beckord, K., Becker, J., and Lutz, H. O. (1995*a*). *Phys. Rev. Lett.* **74**, 1962.

Werner, U., Beckord, K., Becker, J., Folkerts, H. O., and Lutz, H. O. (1995*b*). *Nucl. Instrum. Methods* B **98**, 385.

Werner, U., Kabachnik, N. M., Kondratyev, V. N., and Lutz, H. O. (1997*a*). *Phys. Rev. Lett.* **79**, 1662.

Werner, U., Becker, J., Farr, T., and Lutz, H. O. (1997*b*). *Nucl. Instrum. Methods* B **124**, 298.

Werner, U., Kondratyev, V. N., and Lutz, H. O. (1998). *Nuovo Cimento* A **110**, 1215.

Wohrer, K., and Watson, R. L. (1993). *Phys. Rev.* A **48**, 4784.

Manuscript received 4 November 1998, accepted 7 April 1999